emulsion droplet was less than 23 μm. Figure 4 shows examples of prepared microcapsules. The microcapsules prepared using the emulsion droplets with an average diameter of 5.5 μm, which were prepared using an SPG membrane with a 0.9-μm pore diameter, aggregated three-dimensionally. The microcapsules prepared using the emulsion droplets with an average diameter of 23 μm, which were prepared using an SPG membrane with a 4.8-μm pore diameter, were also aggregated, but they were straightly linked together. In contrast, the microcapsules prepared using the emulsion droplets with an average diameter of 62 μm were dispersed from each other. The structurally organized microcapsules shown in Fig. 4b are very interesting. However, the objective of this paper is the preparation of monodisperse microcapsules. Therefore, we did not pursue why such structurally organized microcapsules occurred. That is left to future work.

To improve the aggregation among individual microcapsules, we investigated the effect of the total surface area of the emulsion droplets on the preparation of monodisperse crosslinked polymelamine microcapsule. In the investigation, the SDS concentration in the mixture of continuous phase I, continuous phase II, and the melamine-formalin pre-polymer solution (the mixture is hereafter called continuous phase III) was 0.1 wt.%. The oil droplet with 13 μm of average diameter was used as the microcapsule core. The emulsion was prepared with 50 cm³ of the oil phase and 200 cm³ of a 0.2-wt.% SDS solution by the SPG membrane emulsification technique. The emulsion was continuously agitated with four flat-blade stirrers at 5 s⁻¹ to maintain homogeneous dispersion of the emulsion droplets. A desired amount of the emulsion was poured into an aqueous solution containing a desired concentration of poly(E-MA) and SDS. The amount of the aqueous phase in the mixture was 100 cm³. The experimental condition was summarized in Table 2 with the ratio of poly(E-MA) amount/the total surface area of the emulsion. The SEM images of the resulting microcapsules are shown in Fig. 5. The aggregation of microcapsules decreased with the decrease of the concentration of the emulsion droplet in the continuous phase III. This result

indicated that the aggregation of microcapsules occurred due to the decrease of poly(E-MA) adsorbed on the surface of the oil droplet. However, as shown in Fig. 5, a large amount of by-produced polymelamine–formaldehyde particles, which were formed in the continuous phase III during microencapsulation, were adhered on the membrane of the microcapsules. The adhesion of the by-produced polymelamine–formaldehyde particle with a large diameter roughens the membrane of the microcapsule. Because SDS strongly affects the increase of the diameter of the by-produced polymelamine–formaldehyde particle as well as the aggregation of the microcapsules, the decrease of SDS concentration in the continuous phase III is essential to prepare monodisperse microcapsule with the smooth membrane.

Subsequently, we investigated the effects of SDS concentration on the aggregation of the microcapsules. The microencapsulation conditions are shown in Table 3. The SDS concentrations in the continuous phase III were adjusted to 0.2, 0.35, and 0.5 wt.% by dissolving different amounts of SDS in continuous phase I. As the capsule core, the emulsion droplet prepared using an SPG membrane with a 4.8-μm pore diameter was used. The average diameter of the emulsion droplets was 23 μm. The prepared microcapsules are shown in Fig. 6. As shown in Figs. 4b and 6, the aggregation of the microcapsules increased remarkably as the SDS concentrations increased. This indicates that the concentration of SDS strongly affects the aggregation of the microcapsules. From these results, we propose the following hypothesis as an effect of SDS on the aggregation of the microcapsules. Poly(E-MA), which is a polymeric surfactant, acts as a protective colloid. It stabilizes an emulsion by electrostatic repulsion and steric repulsion. The steric repulsion, which is caused by the adsorption layer of poly(E-MA) on the surface of an emulsion droplet, would stabilize an emulsion during formation of the microcapsule even if most of the negative charge of poly(E-MA) was cancelled by the melamine–formaldehyde prepolymer and oligomers. On the other hand, SDS stabilizes an emulsion by only the electrostatic repulsion. Because SDS is a surfactant with low molecular weight, a thick adsorption layer is not formed on the surface

Fig. 7 SEM observations of microcapsules prepared in conditions shown in Table 1(B). Average diameters of encapsulated emulsion droplets were a 5.5 μm and b 13 μm. Creamed emulsion was used for microencapsulation
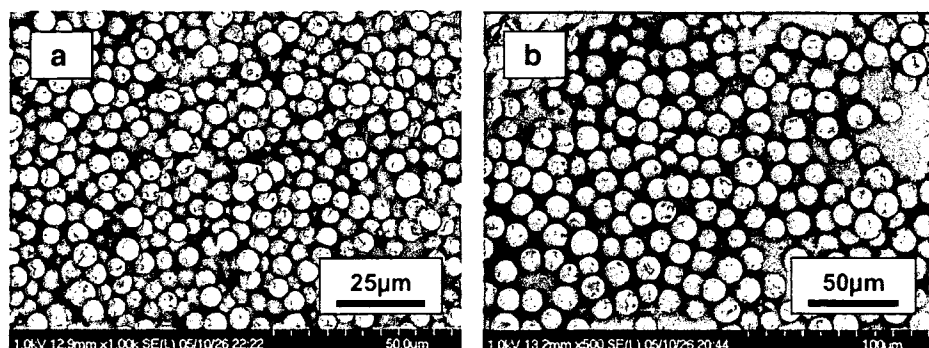
of an emulsion droplet. Therefore, it could not stabilize the emulsion any longer, if the negative charge of SDS was cancelled by the melamine–formaldehyde prepolymer and oligomers. When SDS and poly(E-MA) were co-existed in the continuous phase III, they competitively adsorbed on the surface of the emulsion droplet. An increase of the SDS concentration decreases the adsorption amount of poly(E-MA) on the emulsion droplet. As a result, the poly(E-MA) layer would become thin, and the aggregation of microcapsules occurred. That is to say, it was expected that the well-dispersed crosslinked polymelamine microcapsules with uniform particle size could be prepared by decreasing the SDS concentration in continuous phase III.

To reduce the SDS concentration, we poured the emulsion obtained by SPG membrane emulsification into a separation funnel and creamed it. The lower phase in which the emulsion was not present was dumped. Then, the upper layer was collected and dispersed in continuous phase I. This treatment diluted by about 20 times the SDS concentration in continuous phase III. Figure 7 shows the SEM photographs of crosslinked polymelamine microcapsules prepared using emulsions with 5.5 and 12 μm of the average diameter of oil droplets. The experimental condition is shown in Table 1(B). As expected, the prepared microcapsules were dispersed from each other. The microcapsule diameters and CV values are summarized in Fig. 3. The microcapsule diameter corresponded well to the diameter of the used O/W emulsion droplet. The CV values of the diameter of the prepared microcapsules were also about 10%.

We were able to control the diameter of crosslinked polymelamine microcapsules prepared by phase separation method in the range of 5–60 μm. Microcapsules with different diameters may be prepared by using SPG membranes with different pore diameters.

Conclusion

We investigated the control of the diameter of the crosslinked polymelamine microcapsules. Monodisperse oil droplets prepared by the SPG membrane emulsification technique were used as the capsule core. Monodisperse emulsion droplets with CV value of about 10% were successfully prepared. The average diameter of the emulsion droplets was in proportion to the pore diameter of the SPG membrane. The SDS concentration strongly affected the dispersion stability of the prepared microcapsules. Monodisperse microcapsules were successfully prepared by decreasing the SDS concentration. The diameter of the microcapsule corresponded well to the diameter of the O/W emulsion droplets used as the capsule core. In conclusion, we were able to control microcapsule diameter in the range of 5–60 μm.

References

1. Green BK, Schleicher L (1956) US Patent 2,730,457
2. Comiskey B, Albert JD, Yoshizawa H, Jacobson J (1998) Nature 394:253
3. Wang JP, Zhao XP, Guo HL, Zheng Q (2004) Langmuir 20:10845
4. Kim KS, Lee JY, Park BJ, Sung JH, Chin I, Choi HJ, Lee JH (2006) Colloid Polym Sci 284:813
5. Sawada K, Urakawa H (2005) Dyes Pigm 65:45
6. Park SJ, Shin YS, Lee JR (2001) J Colloid Interface Sci 241:502
7. Brown EN, Kessler MR, Sottos NR, White SR (2003) J Microencapsul 20:719
8. Guo HL, Zhao XP, Wang JP (2005) J Microencapsul 22:853
9. Nakashima T, Shimizu M (1989) Kagaku Kogaku Ronbunshu 15:645
10. Yoshizawa H, Ohta H, Maruta M, Uemura Y, Ijichi K, Hatate Y (1996) J Chem Eng Jpn 29:1027
11. Ma GH, Su ZG, Omi S, Sundberg D, Stubbs J (2003) J Colloid Interface Sci 266:282
12. Supsakulchai A, Ma GH, Nagai M, Omi S (2002) J Microencapsul 19:425
13. Nakashima T, Shimizu M (1993) Kagaku Kogaku Ronbunshu 19:984
14. Omi S, Katami K, Yamamoto A, Iso M (1994) J Appl Polym Sci 51:1
15. Shiomori K, Hayashi T, Baba Y, Kawano Y, Hano T (1995) J Ferment Bioeng 80:552

The First Potent Subtype-Selective Retinoid X Receptor (RXR) Agonist Possessing a 3-Isopropoxy-4-isopropylphenylamino Moiety, NEt-3IP (RXRα/β-dual agonist)

Kayo Takamatsu,[a] Atsushi Takano,[a] Nobumasa Yakushiji,[a] Kazunori Morohashi,[a] Ken-ichi Morishita,[a] Nobuyasu Matsuura,[b] Makoto Makishima,[c] Akihiro Tai,[a] Kenji Sasaki,[a] and Hiroki Kakuta*[a]

Retinoid X receptor (RXR) agonists (rexinoids) are attracting much attention for their use in treatment of cancers, including tamoxifen-resistant breast cancer and taxol-resistant lung cancer, and metabolic disease. However, known RXR agonists have a highly lipophilic character. In addition, no subtype-selective RXR agonists have been found. We previously reported an RXRα-preferential agonist 4-[N-methanesulfonyl-N-(5,5,8,8-tetramethyl-5,6,7,8-tetrahydro-2-naphthyl)amino]benzoic acid (6a). The RXR agonistic activity is much less than that of well-known RXR agonists. To develop potent, less-lipophilic, and subtype-selective RXR agonists, we created new RXR agonists possessing alkoxy and isopropyl groups as a lipophilic domain of the common structure of

well-known RXR agonists. As a result, compounds possessing branched alkoxy groups, 6-[N-ethyl-N-(3-isopropoxy-4-isopropylphenyl)amino]nicotinic acid (NEt-3IP: 7a) and 6-[N-ethyl-N-(3-isobutoxy-4-isopropylphenyl)amino]nicotinic acid (NEt-3IB: 7c), showed RXR agonistic activity as potent as, or more potent than, the activities of representative RXR agonists. Moreover, NEt-3IP (7a) was found to be the first RXRα/β-selective (or RXRα/β-dual) agonist. Being potent, less lipophilic, and having RXR subtype-selective activity, NEt-3IP (7a) is expected to become a new drug candidate and to be a useful biological tool for clarifying each RXR subtype function.

Introduction

Much interest has recently been shown in retinoid X receptors (RXRs) as targets in the treatment of cancers such as tamoxifen-resistant breast cancer and taxol-resistant lung cancer, and metabolic disease.[1–4] RXRs belong to the nuclear receptor superfamily of proteins that regulate many physiological functions in a ligand-dependent manner.[2,5] Nuclear receptors include retinoic acid receptors (RARs), which regulate cell differentiation and proliferation, vitamin D receptor (VDR) which is associated with bone metabolism, and peroxisome proliferator-activated receptors (PPARs), which are associated with lipid metabolism.[2,5,6] Nuclear receptors work as monomers or dimers by themselves or with other partners. Representative nuclear receptors forming heterodimers are RARs, VDR, and PPARs, which function with RXRs.[2,6] Therefore, RXRs are closely linked to the function of such partners, and RXR agonists control synergistically the function of RXR heterodimeric partners.[2,7] RXR agonists are also expected to be dose reducers for RXR heterodimer agonists that possess lipophilic characteristics and can have undesirable side effects owing to their accumulation in adipose tissue or liver.

RXRs have three subtypes (RXRα, β, and γ), which are coded by different genes and are distributed in different locations in the body.[1,2,8] RXRα is expressed mainly in the liver, kidney, and spleen, RXRβ is ubiquitously distributed, and RXRγ is expressed mainly in skeletal muscles, heart muscle, skin, and brain. Figure 1 shows representative endogenous or synthetic RXR

agonists. Endogenous RXR agonists (1, 2) and synthetic RXR agonists (3–5) have a highly lipophilic character and lack of subtype selectivity. Actually, no subtype-selective RXR agonists have been found.[2,9,10] These backgrounds prompted us to create new RXR agonists with low lipophilicity and subtype selectivity.

We have found that reduction of lipophilicity seems to enable production of subtype-selective RXR agonists, and we have discovered a relative subtype-selective RXR agonist 4-[N-methanesulfonyl-N-(5,5,8,8-tetramethyl-5,6,7,8-tetrahydro-2-naphthyl)amino]benzoic acid (6a), which prefers RXRα over

[a] K. Takamatsu, A. Takano, N. Yakushiji, K. Morohashi, K.-i. Morishita,
Prof. A. Tai, Prof. K. Sasaki, Prof. H. Kakuta
Okayama University
Graduate School of Medicine, Dentistry and Pharmaceutical Sciences
1-1-1, Tsushima-Naka, Okayama 700-8530 (Japan)
Fax: (+81) 86-251-7926
E-mail: kakuta@pharm.okayama-u.ac.jp

[b] Prof. N. Matsuura
Faculty of Science
Okayama University of Science
1-1, Ridai-cho, Okayama 700-0005 (Japan)

[c] Prof. M. Makishima
Division of Biochemisty
Department of Biomedical Sciences
Nihon University School of Medicine
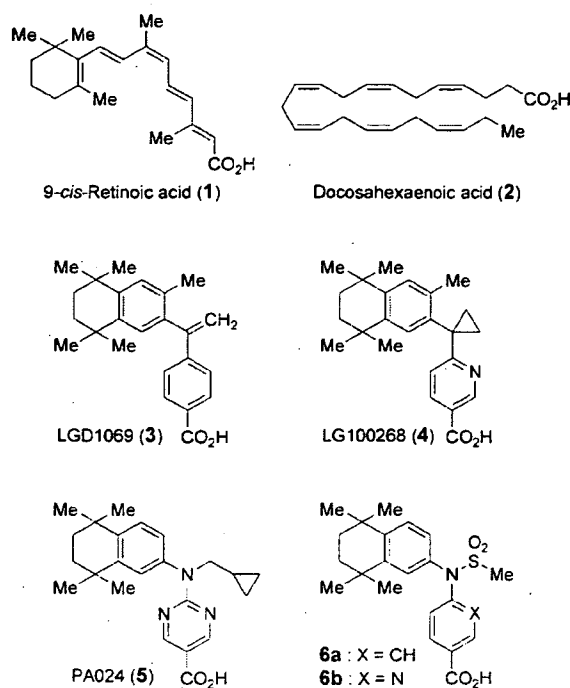30-1 Oyaguchi-kamicho, Itabashi-ku, Tokyo 173-8610 (Japan)

These are not the final page numbers! ↗↗

Figure 1. Chemical structures of known endogenous (1, 2) or synthetic (3–6) RXR agonists.

RXRβ and RXRγ (Figure 1).[11] However, the RXR agonistic activity is much less than that of well-known RXR agonists. The reason for the weak activity is thought to be the introduction of a polar moiety such as a sulfonamide group into the so-called linking group of the common structure of well-known RXR agonists (Figure 2).[11] In this study, we aimed to develop potent, less-lipophilic and subtype-selective RXR agonists. As a result, we discovered 6-[N-ethyl-N-(3-isopropoxy-4-isopropyl-phenyl)amino]nicotinic acid (NEt-3IP: 7a) as the first RXRα/β-selective (RXRα/β-dual) agonist. Herein we report the molecular design and in vitro evaluation.

Design strategy

Our previous results suggest that reduction of lipophilicity at the lipophilc domain of RXR agonists enables production of
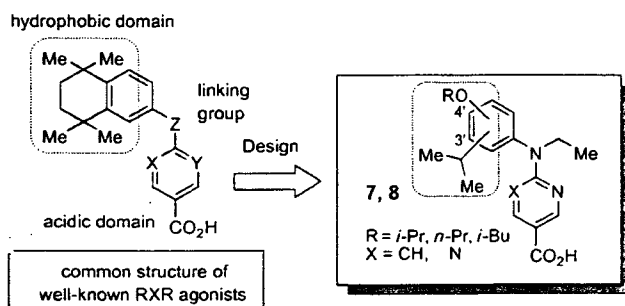

Figure 2. Strategy for the molecular design of subtype-selective RXR agonists possessing alkoxy and isopropyl groups (7, 8).

subtype preference.[11] To develop potent subtype-selective RXR agonists, we replaced a tetramethyl-cyclohexyl ring, the common hydrophobic domain of well-known RXR agonists, with alkoxy and isopropyl groups, which have more polar characteristics. As it was also found that potent RXR activity requires a lipophilic moiety on the linking amino group,[11] N-ethylation was performed for moderate lipophilicity. Nicotinic acid or pyrimidine carboxylic acid was applied to the acidic domain (Figure 2).
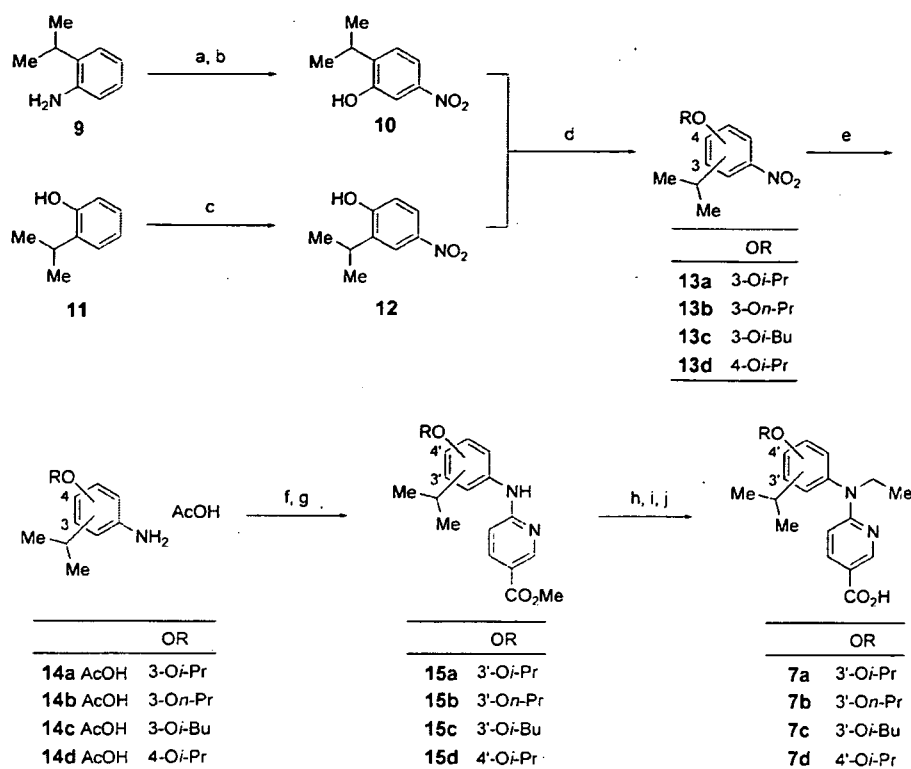
Chemistry

Synthesis was performed by the following steps: synthesis of anilino derivatives, coupling of them with chloronicotinic acid or chloropyrimidine carboxylic acid ester, N-ethylation of the linking amino group, and deprotection of esters. In Scheme 1, synthesis of nicotinic acid derivatives is shown. Anilino derivatives possessing an alkoxy group at the 3-position were prepared by the following procedure: nitration of 2-isopropylaniline with sulfuric acid and nitric acid, replacement of the amino group with a hydroxy group by Sandmyer reaction, O-alkylation with the corresponding alkyl halide, and hydrogen reduction. On the other hand, anilino derivatives possessing an alkoxy group at the 4-position were prepared from 2-isopropylphenol by radical nitration with nitric acid and zinc chloride in an ultrasonic reactor,[12] with similar alkylation and reduction to that described above. The anilino derivatives were reacted with 6-chloronicotinic acid in acetic acid, and the carboxyl groups of the products were protected as methyl ester. After N-ethylation of the linking amino group, deprotection of the methyl ester gave the objective compounds 7a–7d.

Compounds 8a and 8c, whose acidic domains are a pyrimidine-5-carboxylic acid, were prepared via the amino intermediates hydrochloride 14a HCl and 14c HCl according to the reported method (Scheme 2).[13,15] Then N-alkylation and ester deprotection of compounds 16a and 16c were performed to afford the objective compounds 8a and 8c, respectively.

Results and Discussion

RXR agonists alone do not exhibit cell differentiation activity, although they work synergistically with RAR agonists (for example, Am80[10]) to differentiate the human promyelocyte leukemia cell line HL-60 cells to granulocytes.[10,15] This phenomenon is based on the synergistic action of RXR with RAR. For the first screening of the compounds, the activity of compounds alone (retinoid activity) and the activity of compounds with RAR agonists (retinoid synergistic activity) were examined with HL-60.[10,16,17] In this screening, cell differentiation activities were evaluated with nitro blue tetrazolium (NBT) reduction.

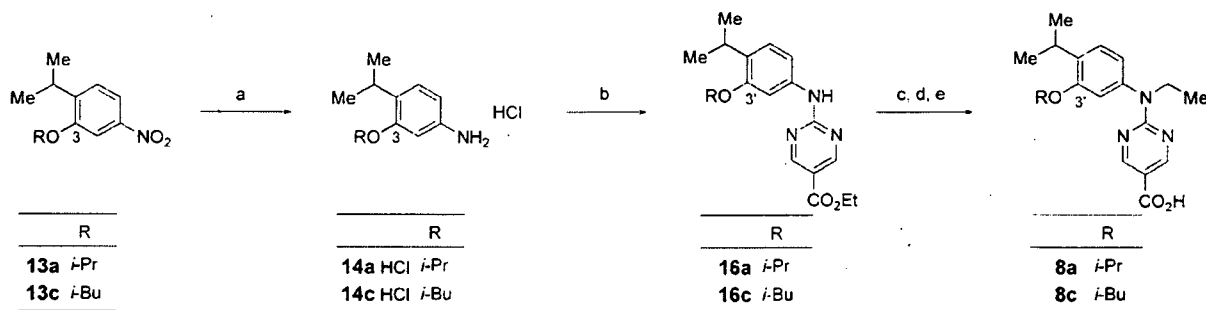First, to examine the proper position of an alkoxy group on the phenylamino moiety, the retinoid and retinoid synergistic activities of NEt-3IP (7a) and NEt-4IP (7d) were assessed (Table 1). Neither of them showed retinoid activities, suggesting that they do not activate RAR directly. On the other hand, retinoid synergistic activities of 7a and 7d were more potent than or as potent as those of sulfonamide-type RXR agonists
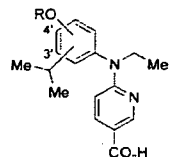
	OR
13a	3-O*i*-Pr
13b	3-O*n*-Pr
13c	3-O*i*-Bu
13d	4-O*i*-Pr

	OR	
14a AcOH	3-O*i*-Pr
14b AcOH	3-O*n*-Pr
14c AcOH	3-O*i*-Bu
14d AcOH	4-O*i*-Pr

	OR
15a	3'-O*i*-Pr
15b	3'-O*n*-Pr
15c	3'-O*i*-Bu
15d	4'-O*i*-Pr

	OR
7a	3'-O*i*-Pr
7b	3'-O*n*-Pr
7c	3'-O*i*-Bu
7d	4'-O*i*-Pr

Scheme 1. Reagents and conditions: a) H_2SO_4, HNO_3. b) $NaNO_2$, H_2SO_4. c) HNO_3, EtOAc, $ZnCl_2$, u-sonic. d) RX, K_2CO_3, DMF. e) H_2, Pd-C, AcOH. f) 6-Chloronicotinic acid, AcOH. g) MeOH, H_2SO_4. h) EtI, NaH, DMF. i) NaOH, MeOH. j) HCl.

retinoid activity similar to that of NEt-3IP (**7a**). The retinoid synergistic activity of NEt-3NP (**7b**) possessing a linear alkoxy group, *n*-propoxy, was less potent than that of NEt-3IP (**7a**) and NEt-3IB (**7c**), suggesting that branched alkoxy groups are appropriate for potent retinoid synergistic activities.

Next, to identify those retinoid synergistic activities exerted via RXR and to compare their potencies toward each RXR subtype, luciferase transcription activities by a reporter gene assay were evaluated.[13,18,19] Table 2 shows their EC_{50} and E_{max} values for each RXR subtype. All of the compounds showed transcription activities, indicating that their retinoid synergistic activities were mediated by RXR. As with the results of the NBT reduction assay, transcription activities of NEt-3IP (**7a**) were found to be more potent than those of NEt-4IP (**7d**). Notably, NEt-3IP (**7a**) and NEt-3IB (**7c**) showed an apparent difference in EC_{50} between each subtype. For NEt-3IP (**7a**), the ratio of EC_{50} (mean values) of RXRα and RXRβ to that of RXRγ was more than tenfold, indicating that this compound prefers RXRα/β over RXRγ. On the other hand, for NEt-3IB (**7c**) the ratio of EC_{50} (mean values) between RXRα:RXRβ:RXRγ was 0.58:23:3, indicating that this compound prefers RXRα over RXRβ. As a more than tenfold difference in EC_{50} values generally indicates the existence of selectivity,[20] it can be assumed that NEt-3IP (**7a**) is an RXRα/β-selective agonist (that is, RXRα/β dual agonist). NEt-3IB (**7c**) has less subtype selectivity than NEt-3IP (**7a**). NEt-3IP (**7a**) has comparable RXR potency to representative potent RXR pan agonists, LGD1069 (**3**) and PA024 (**5**), and NEt-3IB (**7c**) is

6a and 6b, respectively (Table 1). These results suggested that application of alkoxy and isopropyl groups to the hydrophobic domain of RXR agonists enables the production of compounds with retinoid synergistic activities. Notably, the retinoid synergistic activity (SEC_{50} value) of NEt-3IP (**7a**) is 16 ± 1 nM, which is more effective than that of NEt-4IP (**7d**; 135 ± 15 nM). These results prompted us to conclude that the proper position for the introduction of alkoxy is at the 3-position. We therefore investigated the retinoid and retinoid synergistic activities of several derivatives possessing alkoxy groups at the 3-position. NEt-3IB (**7c**) possessing a branched alkoxy group, isobutoxy, was found to show potent retinoid synergistic activity without

	R
13a	*i*-Pr
13c	*i*-Bu

	R
14a HCl	*i*-Pr
14c HCl	*i*-Bu

	R
16a	*i*-Pr
16c	*i*-Bu

	R
8a	*i*-Pr
8c	*i*-Bu

Scheme 2. Reagents and conditions: a) H_2, Pd-C, MeOH, HCl. b) Ethyl 2-chloro-5-pyrimidinecarboxylic acid, K_2CO_3, DMF. c) EtI, NaH, DMF. d) NaOH, EtOH. e) HCl.

These are not the final page numbers! ⟱⟱

Table 1. Cell differentiation-inducing activity of compounds 8–10 by NBT reduction assay.[a]

Compd	OR	Retinoid activity EC$_{50}$ [nM][b]	BA [%][c]	Retinoid synergist activity SEC$_{50}$ [nM][d]	BA [%][c]
NEt-3IP (7a)	3'-O*i*Pr	>1000	n.d.[e]	16±1	83±1
NEt-3NP (7b)	3'-O*n*-Pr	>1000	n.d.	249±16	85±4
NEt-3IB (7c)	3'-O*i*Bu	>1000	n.d.	25±1	81±2
NEt-4IP (7d)	4'-O*i*Pr	>1000	n.d.	135±15	77±4
6a[d]	–	>1000	n.d.	309±33	67±5
6b[d]	–	>1000	n.d.	150±17	73±1

[a] All values were determined from full dose-response curves ranging from 10^{-9} to 10^{-5} M with HL-60 cells. Where errors are indicated, values represent the standard error of the mean value of at least two separate experiments. [b] EC$_{50}$ or SEC$_{50}$ was determined as the concentration of a test compound that required to elicit a response at half-maximal height on the dose-response curve. [c] Biological activity (%) is the maximal differentiation ratio that was induced by a test compound. [d] These data were quoted from reference [11]. [e] Not determinable.

more potent than those representative potent RXR pan agonists. PEt-3IP (8a) and PEt-3IB (8c) showed potent RXR agonistic activities, whereas their subtype selectivity was less than that of NEt series compounds. With increasing polarity of the

acidic domain of the compounds, their RXR agonist activity increased but their subtype selectivity decreased. These results were nearly in accordance with the previous report,[11] suggesting that reduction of the hydrophobic interaction between the hydrophobic domain of the compounds and RXR-ligand binding domain is one strategy to produce subtype selectivity. The CLog*P* value of NEt-3IP (7a) is less than the values of NEt-3IB (7c), LGD1069 (3), and PA024 (5). These results indicate that NEt-3IP (7a) is a potent, less-lipophilic and subtype-selective RXR agonist.

Conclusions

To develop potent, less lipophilic and subtype-selective RXR agonists, we designed new RXR agonists possessing alkoxy and isopropyl groups as a lipophilic domain of the common structure of well-known RXR agonists. As a result, 6-[*N*-ethyl-*N*-(3-isopropoxy-4-isopropylphenyl)amino]nicotinic acid (NEt-3IP: 7a) was discovered as the first RXRα/β-selective agonist. NEt-3IP (7a), being potent and having reduced lipophilicity and RXR subtype-selective activity, is expected to become a new medicinal product and to be a useful biological tool for clarifying each RXR subtype function. In the future, to evaluate the effectiveness of the compound, in vivo studies such as studies on oral absorption, disposition, toxicity, and anticancer activities are being planned.
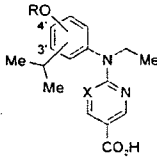
Table 2. Co-transfection data for synthetic compounds and known RXR agonists 3 and 5 in COS-1 cells.[a]

Compd	OR	X	RXRα EC$_{50}$ [nM][b]	E$_{max}$ [%][d]	RXRβ EC$_{50}$ [nM][b]	E$_{max}$ [%][d]	RXRγ EC$_{50}$ [nM][b]	E$_{max}$ [%][d]	Selectivity[e] β/α	γ/α	CLog*P*[f]
NEt-3IP (7a)	3'-O*i*Pr	CH	32±0	136±11	36±8	115±9	376±13	96±6	1.1	11	5.61
NEt-3IB (7c)	3'-O*i*Bu	CH	0.58±0.02	114±4	23±10	140±13	3±1	103±6	39	5.1	6.23
NEt-4IP (7d)	4'-O*i*Pr	CH	410±40	112±11	1180±210	80±4	1430±30	81±15	2.8	3.4	5.61
PEt-3IP (8a)	3'-O*i*Pr	N	9±2	113±4	36±18	103±3	55±15	105±7	4.0	6.1	4.89
PEt-3IB (8c)	3'-O*i*Bu	N	4±2	106±2	5±0	144±14	4±0	105±13	1.2	1.0	5.50
6a[c]	–	–	195±25	115±16	2250±50	52±14	620±50	59±3	11	3.1	6.55
6b[c]	–	–	115±5	98±6	635±75	94±2	350±85	81±7	5.5	3.0	6.13
LGD1069 (3)	–	–	3±0	106±12	6±1	114±12	5±2	104±3	2.0	1.6	8.23
PA024 (5)[d]	–	–	3±1	–	24±0	–	8±1	–	8.0	2.6	7.23

[a] All values represent the standard error of the mean value of at least two separate experiments with triplicate determinations. [b] EC$_{50}$ values were determined from full dose-response curves ranging from 10^{-9} to 10^{-5} M in COS-1 cells. [c] These data were quoted from reference [11]. [d] Luciferase activity of PA024 (5) at 1 μM was defined as 100%. [e] Selectivity was calculated with each EC$_{50}$ value. [f] CLog*P* values were calculated with ChemDraw Ultra7.0.

Experimental Section

Chemistry.

Melting points were determined with a Yanagimoto hot-stage melting point apparatus and are uncorrected. IR were recorded on JASCO FT/IR350 (KBr). ^{1}H NMR spectra were recorded on a VarianVXR-300 (300 MHz) or VarianVXR-500 (500 MHz) spectrometer. Elemental analysis was carried out with a Yanagimoto MT-5 CHN recorder elemental analyzer. FAB-MS was carried out with a VG70-SE.

LGD1069 (3) and PA024 (5). These compounds were prepared according to references <[21] and [13], respectively.

2-Isopropyl-5-nitrophenol (10). Mixed acids (conc. HNO$_3$: conc. H$_2$SO$_4$=2:5, 14 mL) were added to a solution of 2-isopropylaniline 9 (2.7 g, 20 mmol) in conc. H$_2$SO$_4$ (8.0 mL) through a dropping funnel with temperature maintained between −5°C and 0°C. The reaction mixture was alkalinized with 2N NaOH and extracted with EtOAc (3×200 mL). The organic layer was collected, washed with H$_2$O (200 mL) and brine

ЯЯ These are not the final page numbers!

82

(150 mL), and dried over $MgSO_4$. The solvent was evaporated under reduced pressure to yield 2.9 g of 2-isopropyl-5-nitroaniline as brown oil (81%). This compound gave a single spot on TLC, so it was used for the next step without further purification. ${}^1H$ NMR (500 MHz, $CDCl_3$): $\delta = 7.60$ (1 H, dd, $J = 8.5$, 2.5 Hz), 7.50 (1 H, d, $J = 2.5$ Hz), 7.24 (1 H, d, $J = 8.5$ Hz), 3.95 (2 H, br s), 2.90 (1 H, sep, $J = 7.0$ Hz), 1.29 ppm (6 H, d, $J = 7.0$ Hz).

$NaNO_2$ (1.2 g, 18 mmol, dissolved in 3.0 mL of H_2O) was added to a suspension of 2-isopropyl-5-nitroaniline (2.9 g, 16 mmol) in H_2O (3.0 mL) and conc. H_2SO_4 (4.0 mL) with temperature maintained under 5°C. The reaction status was checked by potassium iodide starch test paper. Then the reaction mixture was poured dropwise into a conc. H_2SO_4 (12 mL) and H_2O (9.0 mL) mixture at 120°C. The reaction mixture was poured into H_2O (150 mL) and extracted with EtOAc (3×200 mL). The organic layer was collected, washed with H_2O (200 mL) and brine (150 mL), and dried over $MgSO_4$. The solvent was evaporated under reduced pressure. The residue was purified by flash column chromatography (EtOAc : *n*-hexane = 1:5) to yield **10** as brown oil (2.2 g, 75%). ${}^1H$ NMR (300 MHz, $CDCl_3$): $\delta = 7.78$ (1 H, dd, $J = 8.5$, 2.5 Hz), 7.63 (1 H, d, $J = 2.5$ Hz), 7.33 (1 H, d, $J = 8.5$ Hz), 5.80 (1 H, s), 3.31 (1 H, sep, $J = 7.0$ Hz), 1.28 ppm (6 H, d, $J = 7.0$ Hz).

2-Isopropoxy-1-isopropyl-4-nitrobenzene (13 a). 2-Bromopropane (0.56 mL, 6.0 mmol), K_2CO_3 (552 mg, 3.6 mmol) and KI (catalytic amount) were added to a solution of **10** (668 mg, 3.7 mmol) in dry DMF (4.0 mL). The reaction mixture was stirred at 70°C for 2 h. Then the reaction mixture was poured into H_2O (80 mL) and extracted with EtOAc (3×80 mL). The organic layer was collected, washed with H_2O (2×80 mL) and brine (80 mL), and dried over $MgSO_4$. The solvent was evaporated under reduced pressure. The residue was purified by flash column chromatography to afford **13 a** as light yellow oil (729 mg, 88%). ${}^1H$ NMR (500 MHz, $CDCl_3$): $\delta = 7.76$ (1 H, dd, $J = 8.5$, 2.0 Hz), 7.66 (1 H, d, $J = 2.0$ Hz), 7.31 (1 H, d, $J = 8.5$ Hz), 4.67 (1 H, sep, $J = 6.0$ Hz), 3.36 (1 H, sep, $J = 7.0$ Hz), 1.39 (6 H, d, $J = 6.0$ Hz), 1.22 ppm (6 H, d, $J = 7.0$ Hz).

1-Isopropyl-4-nitro-2-*n*-propoxybenzene (13 b). 1-Iodopropane (595 mg, 3.5 mmol) and K_2CO_3 (414 mg, 3.0 mmol) were added to a solution of **10** (513 mg, 2.8 mmol) in dry DMF (4.0 mL). The reaction mixture was stirred at 80°C overnight. Then the reaction mixture was poured into H_2O (50 mL) and extracted with EtOAc (3× 50 mL). The organic layer was collected, washed with H_2O (2× 50 mL) and brine (50 mL), and dried over $MgSO_4$. The solvent was evaporated under reduced pressure. The residue was purified by flash column chromatography to yield **13 b** as light yellow oil (426 mg, 68%). ${}^1H$ NMR (300 MHz, $CDCl_3$): $\delta = 7.80$ (1 H, dd, $J = 8.5$, 2.5 Hz), 7.65 (1 H, d, $J = 2.5$ Hz), 7.31 (1 H, d, $J = 8.5$ Hz), 4.02 (2 H, t, $J = 6.5$ Hz), 3.39 (1 H, sep, $J = 7.0$ Hz), 1.89 (2 H, m), 1.24 (6 H, d, $J = 7.0$ Hz), 1.09 ppm (3 H, t, $J = 7.5$ Hz).

2-Isobutoxy-1-isopropyl-4-nitrobenzene (13 c). Following the procedure to synthesize **13 a**, **13 c** was obtained in 71% yield as clear yellow oil. ${}^1H$ NMR (300 MHz, $CDCl_3$): $\delta = 7.80$ (1 H, dd, $J = 8.5$, 2.5 Hz), 7.65 (1 H, d, $J = 2.5$ Hz), 7.32 (1 H, d, $J = 8.5$ Hz), 3.82 (2 H, d, $J = 6.5$ Hz), 3.40 (1 H, sep, $J = 7.0$ Hz), 2.17 (1 H, m), 1.25 (6 H, d, $J = 7.0$ Hz), 1.08 ppm (6 H, d, $J = 6.5$ Hz).

3-Isopropoxy-4-isopropylaniline acetate (14 a AcOH). 10% activated Pd-C (catalytic amount) was added to a solution of **13 a** (1.1 g, 4.9 mmol) in AcOH (4.0 mL). The reaction mixture was stirred under H_2 atmosphere at RT for 6 h. The reaction mixture was filtered through celite, and the celite cake was washed with EtOAc (100 mL). The solvent was evaporated under reduced pressure to give **14 a** AcOH (q.y.). This compound gave a single spot on TLC, so it was used for the next step without further purification. ${}^1H$ NMR (500 MHz, $CDCl_3$): $\delta = 6.96$ (1 H, d, $J = 8.0$ Hz) 6.26 (1 H, dd, $J = 8.0$,

2.0 Hz), 6.24 (1 H, d, $J = 2.0$ Hz), 4.46 (1 H, sep, $J = 6.0$ Hz), 3.19 (1 H, sep, $J = 7.0$ Hz), 1.32 (6 H, d, $J = 6.0$ Hz), 1.15 ppm (6 H, d, $J = 7.0$ Hz).

4-Isopropyl-3-*n*-propoxyaniline acetate (14 b AcOH). Following the procedure to synthesize **14 a** AcOH, **14 b** AcOH was obtained (q.y.). This compound gave a single spot on TLC, so it was used for the next step without further purification. ${}^1H$ NMR (300 MHz, $CDCl_3$): $\delta = 7.00$ (1 H, d, $J = 8.0$ Hz), 6.36 (1 H, dd, $J = 8.0$, 2.0 Hz), 6.31 (1 H, d, $J = 2.0$ Hz), 3.87 (2 H, t, $J = 6.5$ Hz), 3.22 (1 H, sep, $J = 7.0$ Hz), 1.81 (2 H, m), 1.17 (6 H, d, $J = 7.0$ Hz), 1.05 ppm (3 H, t, $J = 7.5$ Hz).

3-Isobutoxy-4-isopropylaniline acetate (14 c AcOH). Following the procedure to synthesize **14 a** AcOH, **14 c** AcOH was obtained (q.y.). This compound gave a single spot on TLC, so it was used for the next step without further purification. ${}^1H$ NMR (300 MHz, $CDCl_3$): $\delta = 6.97$ (1 H, d, $J = 8.0$ Hz), 6.27 (1 H, dd, $J = 8.0$, 2.0 Hz), 6.23 (1 H, d, $J = 2.0$ Hz), 3.67 (2 H, d, $J = 6.5$ Hz), 3.22 (1 H, sep, $J = 7.0$ Hz), 2.10 (1 H, m), 1.18 (6 H, d, $J = 7.0$ Hz), 1.04 ppm (6 H, d, $J = 7.0$ Hz).

2-Isopropyl-4-nitrophenol (12). Conc. HNO_3 (2.5 mL, 20 mmol) was added to a solution of 2-isopropylphenol **11** (2.7 g, 20 mmol) in EtOAc (50 mL) in an ice bath. The reaction mixture was placed in an ultrasonic reactor, and $ZnCl_2$ (3.43 g, 25 mmol) was added in small portions over 2.5 h. The reaction mixture was poured into H_2O (100 mL) and extracted with EtOAc (3×100 mL). The organic layer was collected, washed with H_2O (2×100 mL) and brine (100 mL), and dried over $MgSO_4$. The solvent was evaporated under reduced pressure. The residue was purified by flash chromatography to yield **12** (972 mg, 27%) as an off-white solid. ${}^1H$ NMR (300 MHz, $CDCl_3$): $\delta = 8.13$ (1 H, d, $J = 3.0$ Hz), 8.01 (1 H, dd, $J = 9.0$, 3.0 Hz), 6.82 (1 H, d, $J = 9.0$ Hz), 5.74 (1 H, s), 3.25 (1 H, sep, $J = 7.0$ Hz), 1.30 ppm (6 H, d, $J = 7.0$ Hz).

1-Isopropoxy-2-isopropyl-4-nitrobenzene (13 d). Following the procedure to synthesize **13 a**, **13 d** was obtained as brown oil (94%). This compound gave a single spot on TLC, so it was used for the next step without further purification. ${}^1H$ NMR (300 MHz, $CDCl_3$): $\delta = 8.10$ (1 H, d, $J = 3.0$ Hz), 8.07 (1 H, dd, $J = 8.5$, 3.0 Hz), 6.86 (1 H, d, $J = 8.5$ Hz), 4.70 (1 H, sep, $J = 6.0$ Hz), 3.31 (1 H, sep, $J = 7.0$ Hz), 1.40 (6 H, d, $J = 6.0$ Hz), 1.24 ppm (6 H, d, $J = 7.0$ Hz).

4-Isopropoxy-3-isopropylaniline (14 d AcOH). Following the procedure to synthesize **14 a** AcOH, **14 d** AcOH was obtained in crude oil (q.y.). This compound gave a single spot on TLC, so it was used for the next step without further purification. ${}^1H$ NMR (300 MHz, $CDCl_3$): $\delta = 6.71$ (1 H, d, $J = 8.5$ Hz), 6.64 (1 H, d, $J = 3.0$ Hz), 6.53 (1 H, dd, $J = 8.5$, 3.0 Hz), 4.35 (1 H, sep, $J = 6.0$ Hz), 3.28 (1 H, sep, $J = 7.0$ Hz), 1.30 (6 H, d, $J = 6.0$ Hz), 1.17 ppm (6 H, d, $J = 7.0$ Hz).

4-[*N*-(3-Isopropoxy-4-isopropylphenyl)amino]nicotinic acid methyl ester (15 a). 6-Chloronicotinic acid (788 mg, 5.0 mmol) was added to a solution of **14 a** AcOH (1.24 g, 4.9 mmol) in AcOH (4.0 mL). The reaction mixture was stirred at 80°C for 4 h. The reaction mixture was evaporated under reduced pressure. Conc. H_2SO_4 (catalytic amount) was added to a solution of the residue in dry MeOH (5.0 mL) under ice cooling. The reaction mixture was refluxed overnight. The reaction mixture was poured into sat. $NaHCO_3$ (100 mL) and extracted with EtOAc (2×50 mL). The organic layer was collected, washed with H_2O (50 mL) and brine (50 mL), and dried over $MgSO_4$. The solvent was evaporated under reduced pressure. The residue was purified by flash column chromatography to yield **15 a** (702 mg, 44%). ${}^1H$ NMR (300 MHz, $CDCl_3$): $\delta = 8.75$ (1 H, d, $J = 2.5$ Hz), 8.08 (1 H, dd, $J = 9.0$, 2.5 Hz), 7.69 (1 H, br s), 7.19 (1 H, d, $J = 8.0$ Hz), 6.83 (1 H, d, $J = 9.0$ Hz), 6.82 (1 H, d, $J = 2.0$ Hz), 6.81 (1 H, dd, $J = 8.0$, 2.0 Hz), 4.51 (1 H, sep, $J = 6.0$ Hz), 3.90 (3 H, s), 3.32 (1 H, sep, $J = 7.0$ Hz), 1.35 (6 H, d, $J = 6.0$ Hz), 1.21 ppm (6 H, d, $J = 7.0$ Hz).

These are not the final page numbers! ↗↗

83

4-[N-(4-Isopropyl-3-n-propoxyphenyl)amino]nicotinic acid methyl ester (15b). Following the procedure to synthesize **15a**, **15b** was obtained as a purple solid (51% for 2 steps). ^{1}H NMR (300 MHz, CDCl$_3$): $\delta = 8.82$ (1H, d, $J = 2.0$ Hz), 8.03 (1H, dd, $J = 9.0$, 2.0 Hz), 7.18 (1H, d, $J = 8.5$ Hz), 6.89 (1H, s), 6.85 (1H, d, $J = 2.0$ Hz), 6.84 (1H, dd, $J = 8.5$, 2.0 Hz), 6.79 (1H, d, $J = 9.0$ Hz), 3.91 (2H, t, $J = 6.5$ Hz), 3.88 (3H, s), 3.31 (3H, sep, $J = 7.0$ Hz), 1.84 (2H, m), 1.23 (6H, d, $J = 7.0$ Hz), 1.07 ppm (3H, t, $J = 7.5$ Hz).

4-[N-(3-Isobutoxy-4-isopropylphenyl)amino]nicotinic acid methyl ester (15c). Following the procedure to synthesize **15a**, **15c** was obtained as purple solid (62% for 2 steps). ^{1}H NMR (500 MHz, CDCl$_3$): $\delta = 8.82$ (1H, d, $J = 2.5$ Hz), 8.03 (1H, dd, $J = 9.0$, 2.5 Hz), 7.18 (1H, d, $J = 8.5$ Hz), 6.85 (1H, s), 6.84 (1H, dd, $J = 8.5$, 2.0 Hz), 6.83 (1H, d, $J = 2.0$ Hz), 6.79 (1H, d, $J = 9.0$ Hz), 3.89 (3H, s), 3.71 (2H, d, $J = 6.5$ Hz), 3.32 (1H, sep, $J = 7.0$ Hz), 2.13 (1H, m), 1.23 (6H, d, $J = 7.0$ Hz), 1.06 ppm (1H, d, $J = 6.5$ Hz).

6-[N-(4-Isopropoxy-3-isopropylphenyl)amino]nicotinic acid methyl ester (15d). Following the procedure to synthesize **15a**, **15d** was obtained as white solid (57% for 2 steps). ^{1}H NMR (300 MHz, CDCl$_3$): $\delta = 8.75$ (1H, d, $J = 2.5$ Hz), 8.03 (1H, dd, $J = 9.0$, 2.5 Hz), 7.40 (1H, br s), 7.09 (1H, d, $J = 3.0$ Hz), 7.06 (1H, d, $J = 8.0$, 3.0 Hz), 6.85 (1H, d, $J = 8.0$ Hz), 6.67 (1H, d, $J = 9.0$ Hz), 4.54 (1H, sep, $J = 6.0$ Hz), 3.89 (3H, s), 3.32 (1H, sep, $J = 7.0$ Hz), 1.36 (6H, d, $J = 6.0$ Hz), 1.19 ppm (6H, d, $J = 7.0$ Hz).

4-[N-Ethyl-N-(3-isopropoxy-4-isopropylphenyl)amino]nicotinic acid (7a). **15a** (115 mg, 0.35 mmol) was added to a suspension of NaH (16 mg, 0.40 mmol, 60% dispersion in oil) in dry DMF (1.0 mL) at RT under argon. After stirring for 5 min, iodoethane (30 µL, 0.40 mmol) was added, and then it was stirred overnight. The reaction mixture was poured into H$_2$O (20 mL) and extracted with EtOAc (2×10 mL). The organic layer was collected, washed with H$_2$O (10 mL) and brine (10 mL), and dried over MgSO$_4$. The solvent was evaporated under reduced pressure to yield a yellow oil. 2N NaOH (0.50 mL) was added to a solution of the residue in MeOH (2.0 mL), and it was stirred at 60°C for 1 h. The reaction mixture was evaporated under reduced pressure to remove MeOH. The solution was poured into sat. NH$_4$Cl (20 mL) and extracted with EtOAc (3×10 mL). The organic layer was collected, washed with H$_2$O (2×10 mL) and brine (10 mL), and dried over MgSO$_4$. The solvent was evaporated under reduced pressure. Recrystallization from MeOH afforded **7a** as colorless needles (48 mg, 40% for 2 steps). Mp: 212.0–214.0°C; ^{1}H NMR (500 MHz, CDCl$_3$): $\delta = 8.91$ (1H, d, $J = 2.0$ Hz), 7.83 (1H, dd, $J = 9.0$, 2.5 Hz), 7.26 (1H, d, $J = 8.0$ Hz), 6.74 (1H, dd, $J = 8.0$, 2.0 Hz), 6.65 (1H, d, $J = 2.0$ Hz), 6.26 (1H, d, $J = 9.0$ Hz), 4.49 (1H, sep, $J = 6.0$ Hz), 4.06 (2H, q, $J = 7.0$ Hz), 3.32 (1H, sep, $J = 7.0$ Hz), 1.34 (6H, d, $J = 6.0$ Hz), 1.25 (6H, d, $J = 7.0$ Hz), 1.24 ppm (3H, t, $J = 7.0$ Hz); IR (KBr): $v- = 1698$ cm^{-1}; FAB-MS m/z: 343 [M+H]$^+$; Anal. Calcd for C$_{20}$H$_{26}$N$_2$O$_3$: C, 70.15; H, 7.65; N, 8.18. Found: C, 70.18; H, 7.71; N, 8.46.

4-[N-Ethyl-N-(4-isopropyl-3-n-propoxyphenyl)amino]nicotinic acid (7b). Following the procedure to synthesize **7a**, **7b** was obtained as off-white cubics after being recrystallized from CH$_2$Cl$_2$/n-hexane (62% for 2 steps). Mp: 147.0–148.0°C; ^{1}H NMR (300 MHz, CDCl$_3$): $\delta = 8.91$ (1H, d, $J = 2.0$ Hz), 7.86 (1H, dd, $J = 9.0$, 2.0 Hz), 7.28 (1H, d, $J = 8.0$ Hz), 6.76 (1H, dd, $J = 8.0$, 2.0 Hz), 6.64 (1H, d, $J = 2.0$ Hz), 6.29 (1H, d, $J = 9.0$ Hz), 4.13 (2H, q, $J = 7.5$ Hz), 3.88 (2H, t, $J = 6.5$ Hz), 3.35 (1H, sep, $J = 7.0$ Hz), 1.84 (2H, m), 1.27 (3H, t, $J = 7.5$ Hz), 1.26 (6H, d, $J = 7.0$ Hz), 1.07 ppm (3H, t, $J = 7.5$ Hz); IR (KBr): $\bar{v} = 2963$, 1682 cm^{-1}; FAB-MS m/z: 343 [M+H]$^-$; Anal. Calcd for C$_{20}$H$_{26}$N$_2$O$_3$: C, 70.15; H, 7.65; N, 8.18. Found: C, 69.91; H, 7.61; N, 8.13.

4-[N-Ethyl-N-(3-isobutoxy-4-isopropylphenyl)amino]nicotinic acid (7c). Following the procedure to synthesize **7a**, **7c** was obtained as colorless needles after being recrystallized from CH$_2$Cl$_2$/n-

hexane (41% for 2 steps). Mp: 191.5–193.0°C; ^{1}H NMR (300 MHz, CDCl$_3$): $\delta = 8.91$ (1H, d, $J = 2.0$ Hz), 7.83 (1H, dd, $J = 9.0$, 2.0 Hz), 7.26 (1H, d, $J = 8.0$ Hz), 6.77 (1H, dd, $J = 8.0$, 2.0 Hz), 6.64 (1H, d, $J = 2.0$ Hz), 6.25 (1H, d, $J = 9.0$ Hz), 4.04 (2H, q, $J = 7.0$ Hz), 3.68 (2H, d, $J = 6.5$ Hz), 3.36 (1H, sep, $J = 7.0$ Hz), 2.12 (1H, m), 1.26 (6H, d, $J = 7.0$ Hz), 1.25 (3H, t, $J = 7.0$ Hz), 1.06 ppm (6H, d, $J = 6.5$ Hz); IR (KBr): $\bar{v} = 2960$, 1684 cm^{-1}; FAB-MS m/z: 357 [M+H$^+$]; Anal. Calcd for C$_{21}$H$_{28}$N$_2$O$_3$: C, 70.76; H, 7.86; N, 7.92. Found: C, 70.92; H, 7.90; N, 7.89.

4-[N-Ethyl-N-(4-isopropoxy-3-isopropylphenyl)amino]nicotinic acid (7d). Following the procedure to synthesize **7a**, **7d** was obtained as off-white cubics after being recrystallized from n-hexane (54% for 2 steps). Mp: 212.0–214.0°C; ^{1}H NMR (300 MHz, [D$_6$]DMSO): $\delta = 12.45$ (1H, br s), 8.65 (1H, d, $J = 2.5$ Hz), 7.77 (1H, dd, $J = 9.0$, 2.0 Hz), 7.04 (3H, m), 6.14 (1H, d, $J = 9.0$ Hz), 4.93 (2H, q, $J = 7.0$ Hz), 4.64 (1H, sep, $J = 6.0$ Hz), 3.23 (1H, sep, $J = 7.0$ Hz), 1.31 (6H, d, $J = 6.0$ Hz), 1.15 (6H, d, $J = 7.0$ Hz), 1.14 ppm (3H, t, $J = 7.0$ Hz); IR (KBr): $\bar{v} 1664$ cm^{-1}; FAB-MS m/z: 343 [M+H$^+$]; Anal. Calcd for C$_{20}$H$_{26}$N$_2$O$_3$: C, 70.15; H, 7.65; N, 8.18. Found: C, 70.02; H, 7.36; N, 8.23.

3-Isopropoxy-4-isopropylaniline hydrochloride (14a HCl). 10% activated Pd-C (catalytic amount) was added to a solution of **13a** (1880 mg, 8.4 mmol) in MeOH (15 mL). The reaction mixture was stirred under H$_2$ atmosphere at RT for 4 h. The reaction mixture was filtered through celite, and the celite cake was washed with MeOH. The solution was concentrated under reduced pressure. Conc. HCl (0.5 mL) and EtOAc (30 mL) were added to the concentrated solution. The precipitate was filtered to give colorless needles (1915 mg) containing **14a** HCl (99%). ^{1}H NMR (300 MHz, CDCl$_3$): $\delta = 9.84$ (2H, br s), 7.23 (1H, d, $J = 8.0$ Hz), 6.89 (1H, s), 6.81 (1H, d, $J = 8.0$ Hz), 4.53 (1H, sep, $J = 6.0$ Hz), 3.19 (1H, sep, $J = 7.0$ Hz), 1.30 (6H, d, $J = 6.0$ Hz), 1.14 ppm (d, $J = 7.0$ Hz).

3-Isobutoxy-4-isopropylaniline hydrochloride (14c HCl). Following the procedure to synthesize **14a** HCl, **14c** HCl was obtained as colorless needles (89%). ^{1}H NMR (300 MHz, CDCl$_3$): $\delta = 6.98$ (2H, br s), 7.23 (1H, d, $J = 8.0$ Hz), 6.81 (1H, s), 6.80 (1H, d, $J = 8.0$ Hz), 3.73 (2H, d, $J = 6.5$ Hz), 3.22 (1H, sep, $J = 6.5$ Hz), 2.08 (1H, m), 1.16 (6H, d, $J = 6.5$ Hz), 1.02 ppm (6H, d, $J = 6.5$ Hz).

2-[N-(4-Isopropoxy-3-isopropylphenyl)amino]pyrimidine-5-carboxylic acid ethyl ester (16a). K$_2$CO$_3$ (622 mg, 4.5 mmol) and DMF (5 drops) were added to a mixture of 2-chloropyrimidine-5-carboxylate (120 mg, 0.60 mmol) and **14a** HCl (148 mg, 0.60 mmol). The mixture was stirred at 120°C for 12 h. The mixture was poured into 2N HCl (30 mL) and extracted with EtOAc (2×30 mL). The organic layer was collected, washed with H$_2$O (2×30 mL) and brine (20 mL), and dried over MgSO$_4$. The solvent was evaporated under reduced pressure. The residue was purified by flash column chromatography (EtOAc:n-hexane = 1:6) to yield **16a** (152 mg, 69%) as a colorless solid. ^{1}H NMR (500 MHz, CDCl$_3$): $\delta = 8.95$ (2H, s), 7.39 (1H, br s), 7.34 (1H, d, $J = 2.0$ Hz), 7.16 (1H, d, $J = 8.0$ Hz), 6.99 (1H, dd, $J = 8.0$, 2.0 Hz), 4.56 (1H, sep, $J = 6.0$ Hz), 4.37 (2H, q, $J = 7.0$ Hz), 3.28 (1H, sep, $J = 7.0$ Hz), 1.39 (3H, t, $J = 7.0$ Hz), 1.37 (6H, d, $J = 6.0$ Hz), 1.20 ppm (6H, d, $J = 7.0$ Hz).

2-[N-(4-Isobutoxy-3-isopropylphenyl)amino]pyrimidine-5-carboxylic acid ethyl ester (16c). Following the procedure to synthesize **16a**, **16c** was obtained as a colorless solid (33%). ^{1}H NMR (300 MHz, CDCl$_3$): $\delta = 8.95$ (2H, s), 7.46 (1H, s), 7.26 (1H, d, $J = 2.5$ Hz), 7.17 (1H, d, $J = 8.5$ Hz), 7.03 (1H, dd, $J = 8.5$, 2.5 Hz), 4.38 (2H, q, $J = 7.0$ Hz), 3.76 (2H, d, $J = 6.5$ Hz), 3.31 (1H, m), 2.44 (1H, sep), 1.39 (3H, t, $J = 7.0$ Hz), 1.22 (6H, d, $J = 7.0$ Hz), 1.07 ppm (6H, d, $J = 7.0$ Hz).

2-[N-Ethyl-N-(4-isopropoxy-3-isopropylphenyl)amino]pyrimidine-5-carboxylic acid (8a). A solution of **16a** (40 mg, 0.12 mmol) was added to a suspension of NaH (8 mg, 0.20 mmol) in DMF (2.0 mL)

⫝⫝ These are not the final page numbers!

84

under Ar atmosphere. The solution was stirred at RT for 10 min, and then EtI (10 µL, 0.12 mmol) was added, and stirring was continued for an additional 10 min. The solution was poured into H_2O (20 mL) and extracted with EtOAc (2×15 mL). The organic layer was collected, washed with H_2O (2×20 mL) and brine (10 mL), and dried over $MgSO_4$. The solvent was evaporated to yield 38 mg of colorless solid. 2 N NaOH (2.0 mL) was added to a solution of the residue (35 mg, 0.10 mmol) in EtOH (2.0 mL). The mixture was stirred at 60°C for 10 min. The solution was neutralized with 2 N HCl and extracted with EtOAc (2×15 mL). The organic layer was collected, washed with H_2O (2×20 mL) and brine (10 mL), and dried over $MgSO_4$. The solvent was evaporated under reduced pressure to yield **8a** (32 mg, 88% for 2 steps) as a colorless solid. Mp: 197.5–199.0°C; ^1H NMR (300 MHz, $CDCl_3$): $\delta = 8.74$ (2 H, s), 7.21 (1 H, d, $J = 8.0$ Hz), 6.83 (1 H, d, $J = 2.0$ Hz), 6.77 (1 H, dd, $J = 8.0$, 2.0 Hz), 4.56 (1 H, sep, $J = 6.0$ Hz), 4.00 (2 H, q, $J = 7.0$ Hz), 2.11 (1 H, sep, $J = 7.0$ Hz), 1.26 (6 H, d, $J = 6.0$ Hz), 1.19 (6 H, d, $J = 7.0$ Hz), 1.16 ppm (3 H, t, $J = 7.0$ Hz); IR (KBr): $\tilde{v}$1674 cm^{-1}; FAB-MS *m/z*: 344 [M + H$^+$]; Anal. Calcd for $C_{19}H_{25}N_3O_3$: C, 66.45; H, 7.34; N, 12.24. Found: C, 66.38; H, 7.29; N, 12.43.

2-[N-Ethyl-N-(4-isobutoxy-3-isopropylphenyl)amino]pyrimidine-5-carboxylic acid (8c). Following the procedure to synthesize **8a**, **8c** was obtained as colorless needles (69% for 2 steps). Mp: 180.5–182.0°C; ^1H NMR (300 MHz, $CDCl_3$): $\delta = 8.89$ (2 H, s), 7.26 (1 H, d, $J = 8.0$ Hz), 6.79 (1 H, dd, $J = 8.0$, 2.0 Hz), 6.66 (1 H, d, $J = 2.0$ Hz), 4.06 (2 H, q, $J = 7.0$ Hz), 3.69 (2 H, d, $J = 6.5$ Hz), 3.34 (1 H, m), 2.11 (1 H, sep), 1.28 (3 H, t, $J = 7.0$ Hz), 1.25 (6 H, d, $J = 7.0$ Hz), 1.05 ppm (6 H, d, $J = 6.5$ Hz); IR (KBr): v- = 1673 cm^{-1}; Anal. Calcd for $C_{20}H_{27}N_3O_3$: C, 67.20; H, 7.61; N, 11.76. Found: C, 67.01; H, 7.25; N, 11.60.

Calculation of CLogP Values. LogP values for compounds were calculated with ChemDraw Ultra 7.0.

NBT Reduction Assay.

Culture of HL-60 cells. The human promyelocyte leukemia cell line HL-60 was cultured in RPMI1640, which contained 10% fetal bovine serum (FBS) and antibiotics (2% of penicillin-streptomycin solution purchased from SIGMA), in a humidified atmosphere of 5% CO_2 at 37°C.

NBT reduction assay.[10,16,17] Test compounds were dissolved in DMSO at 20 mM for stock solutions. A test compound solution in DMSO was added to a suspension of cells at a concentration of 8× 10^4 cells mL^{-1}. Final DMSO concentration was kept below 0.1%. For vehicle and positive controls, the same volume of DMSO and Am80[8] solution in DMSO were added, respectively. After incubation for 4 days, NBT reduction assay was performed as described below. Cells were incubated in RPMI1640 (10% FBS) and an equal volume of phosphate-buffer saline (PBS (−)) containing 0.2 *w/w*% NBT and 12-*O*-tetradecanoylphorbol-13-acetate (TPA, 200 ng mL^{-1}) in a humidified atmosphere of 5% CO_2 at 37°C for 30 min. The rate of cell differentiation was calculated by the percentage of cells containing blue-black formazan using more than 200 cells. The average of at least three results for each assay was calculated. Synergistic activities of test compounds with Am80 were evaluated in the presence of 3.3×10^{-10} M of Am80, which induces less than 10% of cell differentiation, according to the method described above.

Luciferase Reporter Gene Assay

Culture of COS-1 cells. COS-1 cells were maintained in Dulbecco's modified Eagle's medium supplemented with 10% FBS in a humidified atmosphere of 5% CO_2 at 37°C.

Luciferase reporter gene assay.[13,18,19] Luciferase reporter gene assays were performed using COS-1 cells transfected with three kinds of vectors: each RXR subtype, a luciferase reporter gene under the control of the appropriate RXR response elements, and secreted alkaline phosphatase (SEAP) gene as a background. A CRBPII-tk-Luc reporter and plasmid DNA was purified by a QIA filter Plasmid Midi kit. COS-1 cells were transfected with QIA Effectene Transfection reagent according to the supplier's protocol. Test compound solutions whose DMSO concentrations were below 1% were added to the suspension of transfected cells, which were seeded at about 4×10^4 cells mL^{-1} in 96-well white plates. For vehicle and positive controls, the same volume of DMSO and 9-*cis*RA solution in DMSO were added, respectively. After incubation in a humidified atmosphere of 5% CO_2 at 37°C for 18 h, some of the medium was used for SEAP and the remaining cells were used for luciferase reporter gene assays with a Steady-Glo Luciferase Assay system (Promega) according to the supplier's protocol. The luciferase activities were normalized using secreted alkaline phosphatase (SEAP) activities. The assays were carried out in duplicate three times.

[1] L. Altucci, M. D. Leibowitz, K. M. Ogilvie, A. R. D. Lera, H. Gronemeyer, *Nat. Rev. Drug. Discov.* **2007**, *6*, 793–810.

[2] A. R. de Lera, W. Bourguet, L. Altucci, H. Gronemeyer, *Nat. Rev. Drug. Discov.* **2007**, *6*, 811–820.

[3] C. J. Grubbs, D. L. Hill, K. I. Bland, S. W. Beenken, T.-H. Lind, I. Eto, V. R. Atigadda, K. K. Vines, W. J. Brouillette, D. D. Muccio, *Cancer Lett.* **2003**, *201*, 17–24.

[4] W.-C. Yen, M. R. Corpuz, R. Y. Prudente, T. A. Cooke, R. P. Bissonnette, A. Negro-Vilar, W. W. Lamph, *Clin. Cancer Res.* **2004**, *10*, 8656–8664.

[5] V. Giguére, *Endocr. Rev.* **1999**, *20*, 689–725.

[6] D. J. Mangelsdorf, C. Thummel, M. Beato, P. Herrlich, G. Schütz, K. Umesono, B. Blumberg, P. Kastner, M. Mark, P. Chambon, R. M. Evans, *Cell* **1995**, *83*, 835–839.

[7] D. J. Mangelsdorf, R. M. Evans, *Cell* **1995**, *83*, 841–850.

[8] A. Szanto, V. Narkar, Q. Shen, I. P. Uray, P. J. A. Davies, L. Nagy, *Cell Death Differ.* **2004**, *11*, S126–S143.

[9] P. F. Egea, A. Mitschler, D. Moras, *Mol. Endocrinol.* **2002**, *16*, 987–997.

[10] H. Kagechika, K. Shudo, *J. Med. Chem.* **2005**, *48*, 5875–5883.

[11] K. Takamatsu, A. Takano, N. Yakushiji, K. Morishita, N. Matsuura, M. Makishima, H. I. Ali, E. Akaho, A. Tai, K. Sasaki, H. Kakuta, *ChemMedChem*, in press.

[12] A. Kamal, B. A. Kumar, M. Arifuddin, M. Patrick, *Ultrasonics Sonochemistry* **2004**, *11*, 455–457.

[13] K. Ohta, E. Kawachi, N. Inoue, H. Fukasawa, Y. Hashimoto, A. Itai, H. Kagechika, *Chem. Pharm. Bull.* **2000**, *48*, 1504–1513.

[14] A. Takamizawa, K. Tokuyama, H. Satoh, *Yakugaku Zasshi* 1959, *79*, 664–669.

[15] L. Nagy, V. A. Thomázy, G. L. Shipley, L. Fésüs, W. Lamph, R. A. Heyman, R. A. S. Chandraratna, P. J. A. Davies, *Mol. Cell. Biol.* 1995, *15*, 3540–3551.

[16] S. J. Collins, F. W. Ruscetti, R. E. Gallagher, R. C. Gallo, *J. Exp. Med.* 1979, *149*, 969–974.

[17] T. Takuma, K. Takeda, K. Konno, *Biochem. Biophys. Res. Commun.* 1987, *145*, 514–521.

[18] K. Umesono, K. K. Murakami, C. C. Thompson, R. M. Evans, *Cell* 1991, *65*, 1255–1266.

[19] S. R. Kain, *Methods Mol. Biol.* 1997, *63*, 49–60.

[20] L. Ye, Y.-L. Li, K. Mellström, C. Mellin, L. G. Bladh, K. Koehler, N. Garg, A. M. G. Collazo, C. Litten, B. Husman, K. Persson, J. Ljunggren, G. Grover, P. G. Sleph, R. George, J. Malm, *J. Med. Chem.* 2003, *46*, 1580–1588.

[21] M. F. Boehm, L. Zhang, B. A. Badea, S. K. White, D. E. Mais, E. Berger, C. M. Suto, M. E. Goldman, R. A. Heyman, *J. Med. Chem.* 1994, *37*, 2930–2941.

# FULL PAPERS

The first subtype-selective RXR agonist. NEt-3IP (7a) was found to be the first RXRα/β-selective (or RXRα/β-dual) agonist. Being potent, less lipophilic than previous agonists, and having RXR subtype-selective activity, NEt-3IP (7a) is expected to become a new drug candidate and to be a useful biological tool for clarifying each RXR subtype function.

	EC$_{50}$ [nM]
RXRα	32 ± 0
RXRβ	36 ± 8
RXRγ	376 ± 13
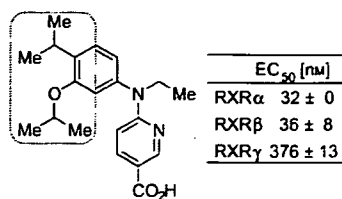
7a (NEt-3IP): RXRα/β-selective agonist

K. Takamatsu, A. Takano, N. Yakushiji,
K. Morohashi, K.-i. Morishita, N. Matsuura,
M. Makishima, A. Tai, K. Sasaki,
H. Kakuta*
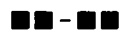
■■ – ■■

The First Potent Subtype-Selective Retinoid X Receptor (RXR) Agonist Possessing a 3-Isopropoxy-4-isopropylphenylamino Moiety, NEt-3IP (RXRα/β-dual agonist)

Hepatic disposition characteristics of Liposomes Coated with Mixture of Hydrophilic Polymers

Tamer Shehata, Ken-ichi Ogawara, Kazutaka Higaki and Toshikiro Kimura

(Division of Pharmaceutical Sciences, Graduate School of Medicine, Dentistry and Pharmaceutical Sciences, Okayama University)

Introduction: Although liposomes are good candidates for efficient drug carriers, the rapid clearance by the reticuloendothelial system (RES) limits their application as drug carriers to other tissues and/or cells. Besides several physicochemical properties of liposomes, such as size, lipid composition and surface charge, certain serum proteins associated onto the surface of liposomes, so-called opsonins, largely influence their hepatic disposition after systemic administration. Surface modification of liposomes by polyethylene glycol (PEG) is known to increase their blood circulation time by inhibiting the interaction of liposomes with opsonins. Recently, lipid-modified polyvinyl alcohol (PVA) is also suggested to be suitable for the same purpose. The objective of this study is to evaluate the biodistribution and hepatic disposition characteristics of liposomes coated with the mixture of PEG and PVA.

Materials and Methods: Liposomes, of which the composition is egg phosphatidylcholine:cholesterol: polymers = 55:40:5 (molar ratio), were prepared by solvent evaporation and hydration method. The resultant liposomes were extruded through a polycarbonate membrane filter and their particle sizes were adjusted around 100 nm. In the in-vivo studies, liposomes labeled with ^{3}H-cholesteryl hexadecyl ether, were intravenously injected into male Wistar rats. Plasma concentrations were determined at different time points and the tissue distribution of liposomes was measured at 6 h after injection. To evaluate the hepatic disposition characteristics of liposomes, single-pass liver perfusion experiments were performed. Furthermore, to analyze the serum proteins associated onto the surface of liposomes, total protein amount was measured and SDS-PAGE analysis was conducted.

Results and Discussion: Liposomes coated with polymer mixture of PEG and PVA (4:1, mol%) (PEG4%/PVA1% liposome) exhibited the highest blood circulating property among liposomes evaluated and showed higher AUC and lower hepatic clearance than any other liposomes including liposomes coated with 5 mol% PEG (PEG5% liposome). These findings were supported by the significantly smaller hepatic disposition of PEG4%/PVA1% liposome than PEG5% liposome in the single-pass liver perfusion experiment. In addition, the pretreatment of perfused liver with trypsin did not affect the hepatic disposition of PEG4%/PVA1% liposome, while the same treatment dramatically decreased that of PEG5% liposomes. These results clearly indicate that the coating of liposome with the mixture of PEG and PVA can avoid the hepatic disposition via the receptor-mediated endocytosis, while the hepatic disposition of PEG5% liposome can mainly be ascribed to the receptor-mediated uptake. On the other hand, the total amount of serum proteins adsorbed on the surface of PEG4%/PVA1% liposome was found to be significantly lower than that for PEG5% liposome. In addition, SDS-PAGE analysis indicated that there was quite large difference in the profiles of serum proteins associated onto these liposomes. These results suggest the decrease in opsonins and/or increase in dysopsonins associated on PEG4%/PVA1% liposome. We are now trying to identify the serum proteins adsorbed on these liposomes. In conclusions, the incorporation of small percentage of PVA into PEG liposome could reduce its affinity to the liver and improve the in-vivo disposition characteristics.

P-糖タンパク質高発現がん細胞に対するドキソルビシン内封 PEG 修飾リポソームの in vivo 抗腫瘍効果に関する検討 (57 字)

運 敬太 [1]、大河原賢一 [1]、西川元也 [2]、
高倉喜信 [2]、檜垣和孝 [1]、木村聰城郎 [1]
[1] 岡山大学 大学院医歯薬学総合研究科 薬学系
[2] 京都大学 大学院薬学研究科

　抗がん剤の長期暴露により、がん細胞表面に高発現する P-糖タンパク質（P-gp）が、抗がん剤の効果を減弱させることが知られている。本研究では、P-gp を高発現する C26 がん細胞を樹立し、ドキソルビシン（DOX）内封 PEG 修飾リポソーム製剤による抗腫瘍効果を in vitro、in vivo 実験系において検討した。樹立したがん細胞の DOX に対する in vitro 感受性は、IC_{50} 値で感受性株の約 200 倍高く、本細胞が DOX に対する耐性を獲得したことが確認された。この耐性株により作製した固形がんモデルマウスに対する DOX 内封 PEG 修飾リポソームの抗腫瘍効果を検討したところ、in vitro 実験系では効果が認められなかったのに対し、in vivo 実験系では感受性株と同程度の高い抗腫瘍効果が認められた。本結果は、耐性株において認められた in vivo 抗腫瘍効果に、DOX のがん細胞に対する直接作用以外の機序が関与している可能性を示唆している。

(420 字)

字数制限
　タイトル：80 字以内
　本文：420 字以内

アルブミン修飾 PEG リポソームの体内動態特性とその抗腫瘍効果の評価

渡　亮輔[1]、寺垣　拓哉[1]、大河原　賢一[1]、横江　淳一[2]、甲斐　俊哉[2]、檜垣　和孝[1]、
木村　聰城郎[1]
1) 岡山大学大学院医歯薬学総合研究科　薬学系
2) ニプロ株式会社　医薬品研究所

　我々はこれまでにポリエチレングリコール（PEG）修飾リポソームの表面にアルブミンを化学的に導入することで、その血中滞留性を増大できることを明らかにしてきた。今回はリモートローディング法によるドキソルビシンの効率的な内封が可能となるアルブミンの結合様式として、リポソーム、アルブミン両者を *N*-succinimidyl 3-(2-pyridyldithio) propionate にて活性化する SPDP 法、及びリポソーム側の活性化には異なるリンカーを使用する改良型 SPDP 法を用いることにより、アルブミン修飾 PEG リポソームを調製し、その静脈内投与後の体内動態特性ならびにドキシルビシンを内封したリポソームの固形がんに対する抗腫瘍効果を評価した。結果、改良型 SPDP 法により調製したアルブミン修飾 PEG リポソームは、その血中滞留性、腫瘍への蓄積性、抗腫瘍効果ともに、SPDP 法で調製したリポソームに比して、顕著に優れていることが明らかとなった。

　　（418 文字）

水酸基を有する高分子安定剤を用いたアニオン分散重合による
単分散ポリ(D,L-乳酸)ミクロスフェアの調製

岡山大院環　〇村中　誠、小野　努

【緒言】　現在、ポリ乳酸(PLA)ミクロスフェアの調製は液中乾燥法が主流である。しかしながら、この手法は予め合成した PLA を用いる多段階プロセスであり、得られる PLA ミクロスフェアの粒径は多分散となる[1]。一方、モノマーからの 1 段階反応である分散重合法は比較的単分散な PLA ミクロスフェアを調製することができる[2]。本研究室では、これまでに重合開始点である水酸基を有する poly(dodecyl methacrylate)-co-poly(2-hydroxylethyl methacrylate) (PDMA-co-PHEMA) (Fig. 1) を高分子安定剤として用いた D,L-ラクチドの分散重合により単分散 PDLLA ミクロスフェアの調製に成功している。本発表では、PDMA-co-PHEMA の分子構造が得られた単分散 PDLLA ミクロスフェアの特性及び生成物形態へ及ぼす影響について報告する。

【実験】　開始剤として過酸化ベンゾイル、溶媒としてトルエンを用いてモノマーである DMA と HEMA を共重合した。得られた PDMA-co-PHEMA は、¹H NMR とゲル浸透クロマトグラフィー (GPC) により分子量、分子量分布、HEMA 導入率(CF)を算出した。

モノマーとして D,L-ラクチド、分散安定剤として PDMA-co-PHEMA を溶解させたキシレン/ヘプタン = 1/2 (v/v) の混合溶液を調製した。その溶液に触媒として 2-エチルヘキサン酸スズ(Ⅱ)を加えて重合した。調製した PDLLA ミクロスフェアは走査型電子顕微鏡により粒径と粒径分散度を測定した。

【結果・考察】 Fig. 2 に得られた PDLLA ミクロスフェアの SEM 写真を示す。Fig. 2 より、平滑な表面を持つ単分散 PDLLA ミクロスフェアであることが確認できた。このことから、分散安定剤として PDMA-co-PHEMA を用いた D,L-ラクチドの分散重合によって単分散 PDLLA ミクロスフェアの調製に成功した。
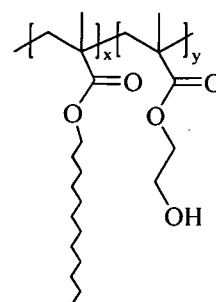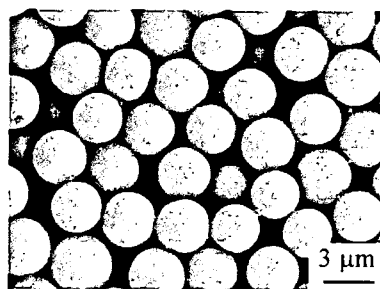

Fig. 1 Chemical structure of PDMA-co-PHEMA

Fig. 2 SEM image of PDLLA microspheres prepared with PDMA-co-PHEMA-A.

Preparation of monodisperse poly(D,L-lactic acid) microspheres by anionic dispersion polymerization using the polymeric stabilizer with hydroxyl groups

Makoto MURANAKA, Tsutomu ONO (Graduate school of Environmental Science, Okayama University, 3-1-1 Tsushima-naka, Okayama 700-8530, Japan)

Tsutomu ONO: Tel&Fax : +81-086-251-8908, E-mail:tono@cc.okayama-u.ac.jp

Key Word: Graft polymeric stabilizer / Anionic dispersion polymerization / Poly(D,L-lactic acid) microspheres / Polymeric micelles

Abstract: Poly(dodecyl methacrylate)-co-poly(2-hydroxylethyl methacrylate) (PDMA-co-PHEMA), copolymer with hydroxyl groups, was synthesized by free radical copolymerization and was used as a stabilizer for the anionic dispersion polymerization of D,L-lactide. The effects of PDMA-co-PHEMA concentration and hydroxyl group number on the particle diameter and polydispersity were examined. In the case of PDMA-co-PHEMA with lower hydroxyl group number, monodisperse PDLLA microspheres were obtained. In contrast, in the case of PDMA-co-PHEMA with higher hydroxyl group number, polymeric micelles were formed.

Table 1 Characteristic parameters of PDMA-*co*-PHEMA and the product for dispersion polymerization

Stabilizer	PDMA-*co*-PHEMA			Product		
	Mw	*Mw/Mn*	*CF* (%)	Morphology	*dp*	*CV* (%)
PDMA-*co*-PHEMA-A	49,380	2.46	1.45	Microsphere	4.53 (µm)	6.14
PDMA-*co*-PHEMA-B	40,851	2.56	6.59	Aggregate	22, 145 (nm)	-
PDMA-*co*-PHEMA-C	40,817	2.35	9.59	Precipitate	-	-

Fig. 3 に PDMA-*co*-PHEMA-A を用いて得られた PDLLA ミクロスフェアと重合後の反応溶液中に存在する高分子安定剤の GPC における溶出曲線を示す。まず、PDLLA ミクロスフェアの溶出曲線は単一ピークを示していることから、精製操作により粒子表面に付着していたほぼ全ての高分子安定剤の除去を確認した。通常、分散重合法の欠点として微粒子表面に存在する高分子安定剤の除去が困難である。しかしながら、本重合系においては純粋な PDLLA ミクロスフェアを調製することができた。また、重合後の反応溶液中に存在する高分子安定剤の分子量は用いた PDMA-*co*-PHEMA よりも高分子量側にシフトしていた。このため、PDMA-*co*-PHEMA 構造中の水酸基から D,L-ラクチドの重合の進行が示唆された。

Table 1 は HEMA 導入率の異なる 3 種類の PDMA-*co*-PHEMA の分子構造と、それらを用いて得られた生成物の形態とその特性を示す。HEMA 導入率の最も小さい PDMA-*co*-PHEM-A を用いた場合には PDLLA ミクロスフェアが得られた。次に、PDMA-*co*-PHEM-B を用いた場合は、反応溶液は白濁することなく、半透明な溶液で得られた。この反応溶液を動的光散乱 (DLS) 測定した結果を Fig. 4 に示す。Fig. 4 より、二峰性ピークの存在が明らかとなり、反応溶液中で高分子会合体を形成していることが示唆された。PDMA-*co*-PHEM-C を用いた場合には、反応中に大きなバルク状の塊が析出した。この析出物の ¹H NMR スペクトルを Fig. 5 に示す。Fig. 5 より、PDLLA と PDMA 由来の両ピークの存在を確認したため、この析出物が PDMA-*co*-PHEMA-*co*-P(MA-PDLLA)であることを同定した。今回の検討から、PDMA-*co*-PHEMA 構造中の HEMA 導入率を変化させることで、様々な形態をとる生成物を調製できることが明らかとなった。

【引用文献】

[1] G. Ma, M. Nagai, O. Shinzo, *J. Colloid Surfaces A*, **153**, 383 (1999).

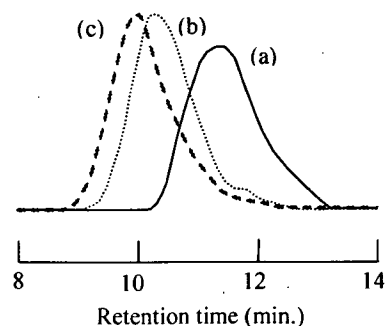[2] S. Sosnowski, M. Gadzinowski, S. Slomkowski, S. Penczek, *J. Bioactive Compatible Polym.*, **9**, 345 (1994)

Fig. 3 GPC traces of (a) prepared PDLLA microspheres, (b) PDMA-*co*-PHEMA-A, (c) PDMA-*co*-PHEMA-*co*-P(MA-PDLLA)-A.
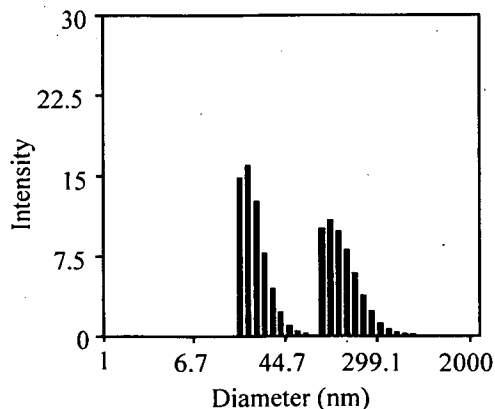

Fig. 4 DLS histogram of the reaction solution after the dispersion polymerization of D,L-lactide using PDMA-*co*-PHEMA-B.
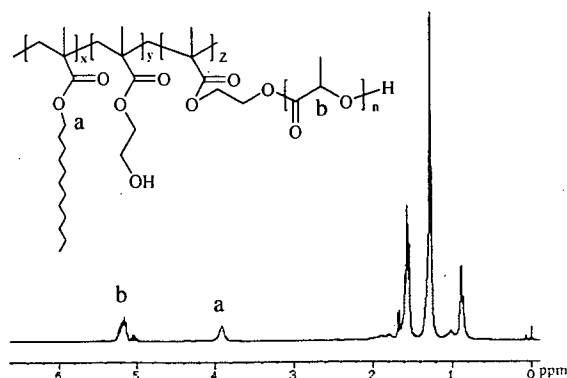

Fig. 5 ¹H NMR spectrum of the precipitate obtained from the dispersion polymerization of D,L-lactide using PDMA-*co*-PHEMA-C.

Time-Dependent Changes in Opsonin Amount Associated on Nanoparticles Alter Their Hepatic Uptake Characteristics

Ken-ichi Ogawara, Susumu Nagayama, Kazutaka Higaki and Toshikiro Kimura

Division of Pharmaceutical Sciences, Graduate School of Medicine, Dentistry and Pharmaceutical Sciences, Okayama University, 1-1-1 Tsushima-naka, Okayama 700-8530, Japan

Utilization of nanoparticulate drug carriers is one of the promising approaches to achieve the organ specific drug delivery. Intravenously injected nanoparticles first contact and associate with serum proteins including opsonins which are recognized by their specific receptors on macrophages in reticuloendothelial system, especially in the liver and spleen. This process, so-called opsonization, leads to the rapid elimination of nanoparticles from the blood circulation, which has limited the clinical application of nanoparticulate drug carriers so far. To understand and/or improve their in-vivo disposition, the interaction of nanoparticles with serum proteins has been intensively investigated. Although there are many papers describing the relationship between the opsonin amounts associated on the surface of particles and their affinity to the liver, there is no report investigating whether the time-dependent change in the adsorption profile of serum proteins on nanoparticles substantially alters the hepatic disposition or not. Therefore, in the present study, we investigated the correlation between the time-dependent change in the adsorption pattern of serum proteins on lecithin-coated polystyrene nanoparticle with a size of 50 nm (LNS-50), used as a model nanoparticle, and its disposition characteristics to the liver. The total amount of proteins adsorbed on LNS-50 increased and the qualitative profile of serum proteins adsorbed on LNS-50 changed during the incubation with serum up to 360 min. The liver perfusion study indicated that the hepatic uptake of LNS-50 incubated with serum for 360 min was significantly larger than those of LNS-50 incubated for shorter periods. Semi-quantification of major opsonins, complement C3 (C3) and immunoglobulin G (IgG), and in-vitro uptake study in primary cultured Kupffer cells demonstrated that the increase in C3 and IgG amounts adsorbed on LNS-50 was directly reflected in the increased disposition of LNS-50 to Kupffer cells. In addition, the amounts of some other opsonins that are known to enhance the uptake of nanoparticles by hepatocytes also increased over incubation time periods, which would be responsible for the time-dependent change in the in-vitro uptake characteristics of LNS-50 by hepatocytes. These results demonstrated that the amounts of opsonins associated on nanoparticles would change over time and this process would be substantially reflected in the alteration of their hepatic disposition characteristics.

In Vivo Anti-Tumor Effects of PEG-Modified Liposomal Doxorubicin on P-Glycoprotein Over-Expressing Tumor-Bearing Mice

Keita Un[a], Takaaki Nakao[a], Ken-ichi Ogawara[a], Makiya Nishikawa[b], Yoshinobu Takakura[b], Kazutaka Higaki[a] and Toshikiro Kimura[a]

a) Division of Pharmaceutical Sciences, Graduate School of Medicine, Dentistry and Pharmaceutical Sciences, Okayama University, 1-1-1 Tsushima-naka, Okayama 700-8530, Japan
b) Department of Biopharmaceutics and Drug Metabolism, Graduate School of Pharmaceutical Sciences, Kyoto University, Sakyo-ku, Kyoto 606-8501, Japan

The resistance of cancer cells to various anti-cancer drugs such as doxorubicin (DOX) has been clinically observed and the effectiveness of these drugs gradually decreases during treatment. Multidrug resistance is, therefore, one of the greatest concerns in cancer chemotherapy. It has been considered that the over-expression of P-glycoprotein (P-gp), known as the multidrug efflux pumps, plays a key role in the tumor acquisition of multidrug resistance by inhibiting intracellular accumulation of drug. In the present study, we established the DOX-resistant colon-26 cancer cells (C26/DOX) and evaluated the *in vitro* cytotoxic effect and *in vivo* therapeutic effect of polyethylene glycol (PEG)-modified liposomal DOX for C26/DOX. First of all, we examined the *in vitro* sensitivity of C26/DOX to DOX. IC_{50} value (40 µM) for C26/DOX was about 250-fold larger than that (0.15 µM) of control C26 (C26/control), demonstrating that C26/DOX was much more resistant to DOX. Western blot analysis confirmed the over-expression of P-gp in C26/DOX. The addition of verapamil, known as a P-gp blocker, to the medium dramatically potentiated the cytotoxic effect of DOX to C26/DOX. On the other hand, PEG liposomal DOX was not able to overcome the resistance of C26/DOX in the *in vitro* study. Then, we evaluated the *in vivo* therapeutic effect of PEG liposomal DOX by measuring the tumor volume in the C26/DOX- or C26/control-bearing mice. Unexpectedly, contrary to the *in vitro* studies, PEG liposomal DOX was significantly effective for both C26/DOX- and C26/contol-bearing mice in terms of the extent of tumor growth inhibition. As the *in vivo* tumor accumulation of PEG liposome and the microvessel density within tumors were similar in both C26/DOX- and C26/contol-bearing mice, other mechanisms except the direct effect of DOX to tumor cells would be responsible for the *in vivo* anti-tumor effect of PEG liposomal DOX in C26/DOX-bearing mice. Therefore, we focused on the endothelial cells surrounding angiogenic vessels within the tumor. IC_{50} value of DOX in human umbilical vein endothelial cells (HUVEC), widely used as a model of angiogenic vascular endothelial cells, was found to be 0.16 µM, and this value was similar to that in C26/control. We are now trying to elucidate the substantial role of cytotoxic effect of DOX to endothelial cells in C26/DOX-bearing mice. (2367 letters, 366 words)

332p Phase Inversion Temperature (Pit) Method Utilized Preparation Of O/w Nano-Emulsion By Microreactor System

Jun Kubota[1], Aiko Kato, and Tsutomu Ono[2]. (1) Department of Environmenta Chemistry and Material, Okayama University, 3-1-1, Tsushima-naka, Okayama, Japan, (2) Department of Material & Energy Science, Okayama University, 3-1-1, Tsushima-naka, Okayama, Japan

O/W Nano-emulsion was successfully prepared by applying microreactor system in water/polyethylene glycol dodecyl ether (C12E4)/dodecane system by the phase inversion temperature method. Nano-emulsification was carried out by combining two consecutive microreactors. Initially, relatively large droplets were prepared in Y-shaped microchannel as pre-emulsification with distilled water as the continuous phase (flow rate; 100 μl/min.) and 20 wt% C12E4-80 wt% dodecane solution as the disperse phase (flow rate; 40 μl/min.). Immediately after that, prepared pre-emulsion was heated up to 333 K by passing through in a tubular microreactor. According to the standard recipe, time required to heat up at 333 K was measured to be 12.6 s. Heated solution was then cooled by air (298 K) to obtain nano-emulsion (droplet diameter; ca 100 nm, measured by dynamic light scattering (DLS)). Stability of the nano-emulsion was also investigated by measurement of the droplet diameter as a function of time. The results showed that the droplet diameter slightly increased from 90 to 120 nm with the elapse of time (up to 100 h). Furthermore, the noble estimation procedure was confirmed to design the suitable microreactor for nano-emulsification by the phase inversion temperature method. These investigations show the great potential for continuously preparing the monodispersed nano-emulsion, and can be expected to apply the pharmaceutical and cosmetic field.

ポリアスパラギン酸ナトリウムを主鎖に持つマクロモノマーを用いた高分子微粒子の調製

（岡山大院環境学） ○冨田恵介・小野 努

[緒言] 表面に機能性高分子鎖を持つ微粒子は様々な応用への展開が期待される先端材料の一つである。反応性官能基を持つ高分子（マクロモノマー）を用いた分散共重合化共重合はワンポットで表面に高分子鎖を持つ高分子微粒子の調製が可能な重合プロセスとして知られている。本研究では、側鎖にビニル基を持つポリアスパラギン酸ナトリウムマクロモノマー(VBA-PAspNa; Fig. 1)を用いたスチレンとの分散共重合を行い、重合挙動に及ぼす各種重合パラメーターの影響について検討した。

[実験] 本実験にはビニル基割合 10 mol%の VBA-PAspNa(重合度=307)を用いた。開始剤(2',2'-アゾビスイソブチロニトリル)、モノマー(スチレン)、VBA-PAspNa をエタノール・水の混合溶媒（エタノール/水=3/2）に溶解させた。この溶液を反応器内に入れ、窒素置換後、343 K で 6 時間反応させた。得られた微粒子の SEM 観察により平均粒径を求め、粒径分布の指標となる CV(=標準偏差/平均粒径×100)を算出した。スチレンモノマー重合率は高速液体クロマトグラフィーにより測定した。粒子数は平均粒径と重合率から算出した。

[結果と考察] 異なるスチレンモノマー濃度での VBA-PAspNa を用いたスチレンの分散共重合における粒子数・CV の経時変化を Fig. 2 に示す。重合初期に粒子数と CV の増加が確認された。また、スチレンモノマー濃度の増加に伴い、CV および粒子数の増加期間は長くなることがわかった。この粒子数と CV の増加は新生粒子の形成によるものであり、モノマー濃度の増加が新生粒子の形成を促進していることを示す。生成した粒子の表面は VBA-PAspNa で覆われており、スチレンオリゴマーの取り込みは抑制される。すなわち、新粒子の形成は均相で形成されるスチレンオリゴマーが既存の粒子に取り込まれずに析出・凝集したためであると推察される。他の重合パラメーターの影響については発表にて詳しく説明する。
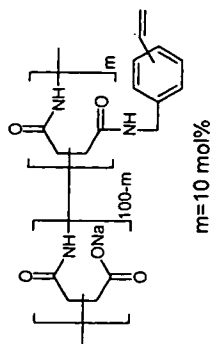
○とみたけいすけ・おのつとむ

Fig. 1 Chemical structure of VBA-PAspNa

m=10 mol%

[Styrene] (g/ml)
◆ 1.49×10⁻² △ 4.47×10⁻²
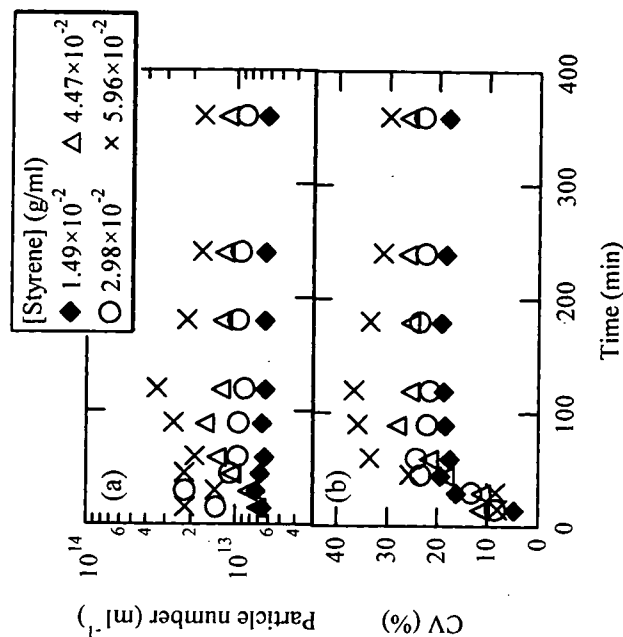○ 2.98×10⁻² × 5.96×10⁻²

Fig. 2 Time course of (a) particle number, (b) CV in dispersion copolymerization with various concentration of styrene monomer.